Development of a one-dimensional Wolter mirror for an advanced Kirkpatrick–Baez mirror

S. Matsuyama*[a], T. Wakioka[a], H. Mimura[a], T. Kimura[a], N. Kidani[a], Y. Sano[a], Y. Nishino[b], K. Tamasaku[c], M. Yabashi[c], T. Ishikawa[c], K. Yamauchi[a,d]
[a] Department of Precision Science and Technology, Graduate School of Engineering, Osaka University, 2-1 Yamada-oka, Suita, Osaka 565-0871, Japan
[b] Research Institute for Electronic Science, Hokkaido University, Kita 21 Nishi 10, Kita-ku, Sapporo 001-0021, Japan
[c] RIKEN/SPring-8, 1-1-1 Kouto, Sayo-cho, Sayo-gun, Hyogo 679-5148, Japan
[d] Research Center for Ultra-Precision Science and Technology, Graduate School of Engineering, Osaka University, 2-1 Yamada-oka, Suita, Osaka 565-0871, Japan

ABSTRACT

To realize achromatic full-field hard X-ray microscopy with a resolution better than 100 nm, we studied an imaging system consisting of an elliptical mirror and a hyperbolic mirror. The figure accuracies of the elliptical and hyperbolic mirrors required to obtain diffraction-limited resolution were investigated using a wave-optical simulator, and then elliptical and hyperbolic mirrors were precisely fabricated, following the criterion of the figure accuracies. Experiments to form a demagnified image of a one-dimensional slit installed 45 m upstream were conducted using the imaging system at an X-ray energy of 11.5 keV at BL29XUL of SPring-8. The system could form a demagnified image with the best resolution of 78 nm. In addition, the field of view to obtain a resolution better than 200 nm was 4.2 micron.

Keywords: Advanced Kirkpatrick-Baez mirror, Wolter mirror, full-field X-ray microscopy, X-ray mirror

1. INTRODUCTION

High-performance imaging devices are required to construct a full-field hard X-ray microscope with a high resolution. Fresnel zone plates (FZPs) are currently the most suitable devices for high-resolution microscopy because they can be fabricated with an external zone of better than 30 nm[1]. However, they can't be utilized for spectromicroscopy such as full-field X-ray fluorescence microscopy because of chromatic aberration. Another promising device is a Wolter mirror[2] that consists of an elliptical mirror and a hyperbolic mirror having an axially symmetric shape, because total reflection allows achromatic and efficient imaging. However, Wolter mirrors that are sufficiently accurate to realize diffraction-limited resolution have never been fabricated because figuring an axially symmetric aspherical shape on the inner tube is very challenging for engineers even if ultraprecision machining and measuring are utilized.

P. Kirkpatrick and A. V. Baez have proposed a two-mirror system (known as a Kirkpatrick–Baez mirror) to form an image using nearly planar mirrors[3]. In this system, two concave mirrors that are orientated perpendicular to each other are used to form a two-dimensional image. R. Kodama et al. developed a four-mirror system to expand a field of view (FOV) and termed it the advanced Kirkpatrick–Baez (AKB) mirror[4]. It consists of a pair of one-dimensional Wolter mirrors each consisting of an elliptical mirror and a hyperbolic mirror. They used this system to construct an X-ray microscope with a spatial resolution of better than 3 μm at an X-ray energy of ~2.5 keV.

This arrangement has the potential to realize high-resolution X-ray microscopy because figuring nearly planar mirrors is relatively straightforward compared with figuring an axially symmetric aspherical shape and it allows the imaging device to avoid a wavefront aberration that degrades a spatial resolution. So we have investigated an AKB mirror to realize a full-field hard X-ray microscope with a resolution of better than 100 nm (Fig. 1). In the present study, the figure accuracies of the elliptical and hyperbolic mirrors required to obtain diffraction-limited resolution were investigated using

*matsuyama@prec.eng.osaka-u.ac.jp; phone/fax +81-6-6879-7286; http://www-up.prec.eng.osaka-u.ac.jp/eng/index.htm

Advances in X-Ray/EUV Optics and Components V, edited by Ali M. Khounsary, Christian Morawe, Shunji Goto,
Proc. of SPIE Vol. 7802, 780202 · © 2010 SPIE · CCC code: 0277-786X/10/$18 · doi: 10.1117/12.860405

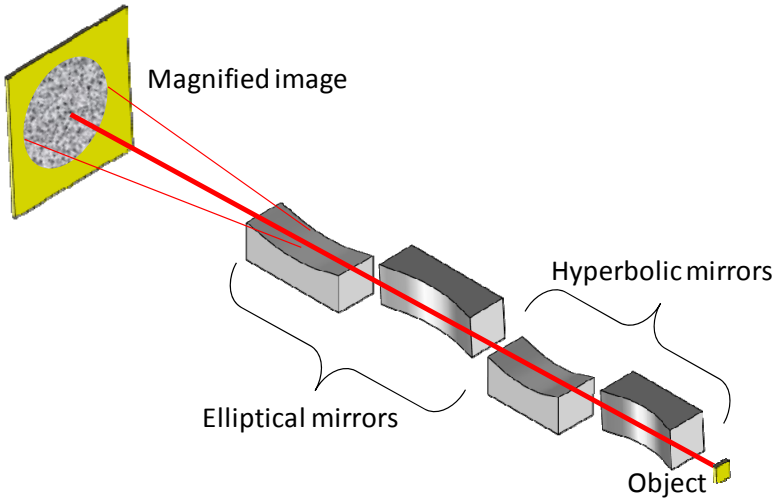

Figure 1 Arrangement of an advanced Kirkpatrick–Baez mirror. In this paper, only a one-dimensional Wolter mirror near the object is discussed.

a wave-optical simulator and a one-dimensional Wolter mirror was actually constructed. A demagnified image of a one-dimensional slit installed 45 m upstream was observed at an X-ray energy of 11.5 keV at BL29XUL of SPring-8.

2. ONE-DIMENSIONAL WOLTER MIRROR

2.1 Design

Two elliptical figures and two hyperbolic figures in the AKB mirror were optimally designed under the following conditions; the microscope has a diffraction-limited spatial resolution with a full width at half maximum (FWHM) of less than 45 nm and a working distance of 50 mm, and can effectively form an image at the experimental hutch 2 (EH2) of BL29XUL[5] of SPring-8 at an X-ray energy of 11.5 keV. In this case, 12 parameters including mirror lengths, glancing angles and focal lengths of the four mirrors were decided. Table 1 summarizes the parameters of the two mirrors discussed in this paper and the mirror figures and slopes are shown in Fig. 2. The geometrical arrangement used is illustrated in Fig. 3. The optical setup, which functions as a demagnification imaging system, was employed to evaluate a point spread function of the Wolter mirror.

Table 1 Parameters of designed elliptic and hyperbolic mirrors

	Elliptical mirror	Hyperbolic mirror
a (m)*	22.75	10.84×10^{-3}
b (m)*	58.46×10^{-3}	0.5437×10^{-3}
Active mirror length (m)	125×10^{-3}	29×10^{-3}
glancing angle at the center (rad)	2.8×10^{-3}	5.0×10^{-3}
Distance from a source (m)**	45.17	45.32
Distance from a focus point (m)**	215×10^{-3}	65×10^{-3}
Working distance (m)	50×10^{-3}	
Diffraction limited FWHM (nm)***	43	

*Elliptical mirror: $x^2/a^2+y^2/b^2=1$, Hyperbolic mirror: $x^2/a^2-y^2/b^2=1$
**The distance from each point to a center of the mirror
***At an X-ray energy of 11.5 keV

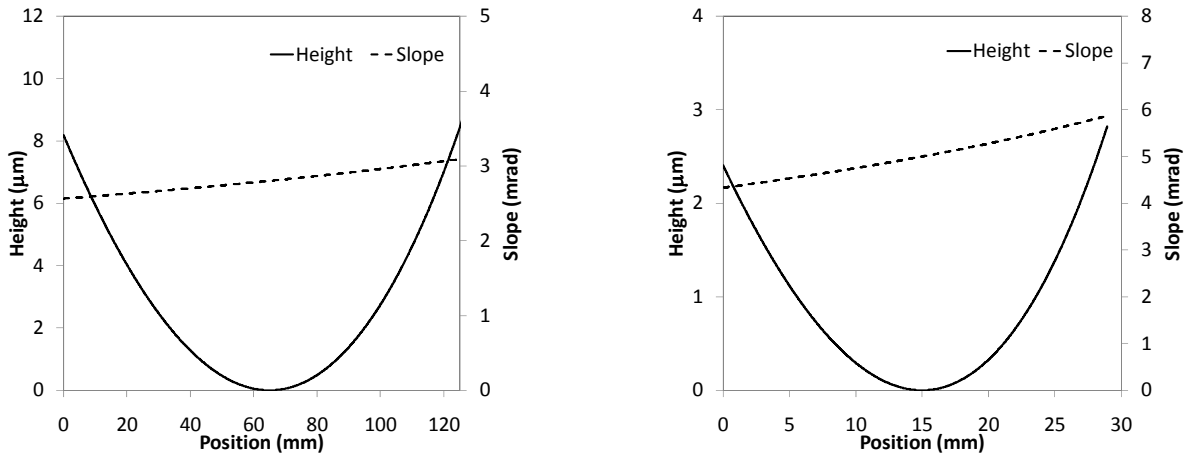

(a) Elliptical mirror (b) Hyperbolic mirror

Figure 2 Figures and slopes of designed mirrors

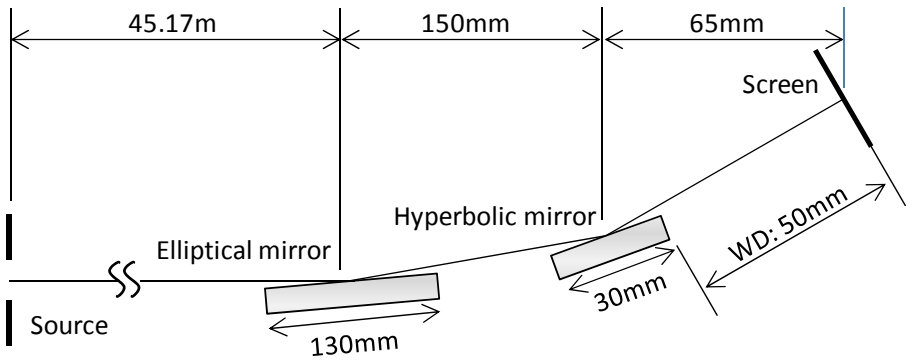

Figure 3 Geometrical arrangement of the designed one-dimensional Wolter mirror. It can form a demagnified image of the slit on the screen.

2.2 Simulation for investigating the required figure accuracy

To investigate the figure accuracy required for the designed mirrors, the X-ray intensity distributions in the focal plane under several conditions were calculated using a wave-optical simulator, which is based on the Fresnel–Kirchhoff's diffraction integral. Details of the calculation are described elsewhere[6,7]. The calculation contains the effect of refractivity on the glancing angles and surface roughness at an X-ray energy of 11.5 keV. The root mean square (RMS) surface roughness for all spatial frequencies on both mirrors was taken to be 0.5 nm. X-ray energy was set to 11.5 keV. All the simulations used the geometrical arrangement of the designed one-dimensional Wolter mirror. The source size was set to 10 μm, which can be assumed to be a point source.

Image profiles at the screen were investigated with figure errors modeled by sinusoidal curves. Sine functions having spatial frequencies in the range 2–128 WAVE (here, WAVE is defined as the number of sine waves per mirror length) and amplitudes of 1–3 nm were considered. The behaviors of satellite peaks were analyzed because these peaks reduce the spatial resolution of a microscope. The relationship between the figure error spatial frequency and the absolute position of the satellite peaks for a sine amplitude of 2.5 nm is shown in Fig. 4(c). This result shows that the spatial frequency of the figure error affects the positions of the satellite peaks. In this case, the FWHM of the main peak was hardly changed. This result can be explained in terms of simple diffraction theory based on the Fourier transform because X-rays scattered by the mirror surfaces are focused on the focal plane. Additionally, the relationship between the spatial frequency and the ratio of the satellite peak intensities to the main peak intensity were calculated for sine curves having amplitudes of 1, 2 and 3 nm (Fig. 5). The intensity ratios were affected by not only heights of the figure error, but also spatial frequency. Moreover, the hyperbolic mirror was sensitive to the figure error compared with the elliptical

mirror. This is because the glancing angle of the hyperbolic mirror was 1.8 times larger than that of the elliptical mirror at the center of each mirror. According to the Bragg equation, the phase shift (Θ, rad) of an X-ray beam reflected on a bump site (such as a figure error) is described by:

$$\Theta = 2\pi \cdot \frac{2d \cdot \sin\theta}{\lambda} \qquad (1)$$

where d is the height of the bump, θ is the glancing angle and λ is the X-ray wavelength. Thus, the hyperbolic mirror needs to be figured 1.8 times more precisely than the elliptical mirror. Simulation results suggest that the hyperbolic mirror should be fabricated with a Peak-to-Valley figure accuracy of 2 nm, especially in the spatial frequency range lower than 8 WAVE, and the elliptical mirror should be fabricated with a Peak-to-Valley figure accuracy of 4 nm, especially in the range lower than 8 WAVE.

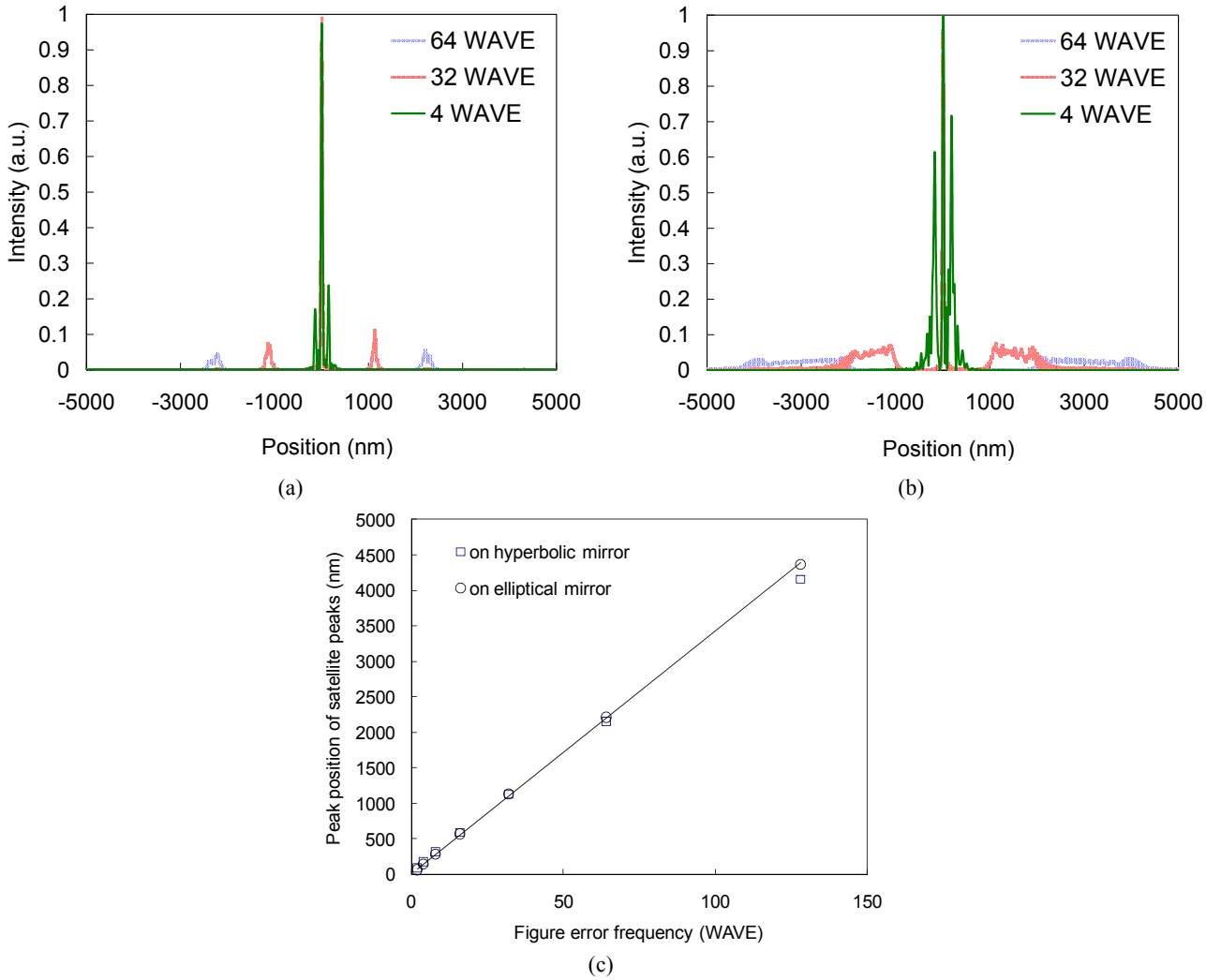

Figure 4 Satellite peaks produced by figure errors on (a) the elliptical and (b) the hyperbolic mirrors, and (c) the relationship between the figure error frequency and the absolute position of satellite peaks for a sine amplitude of 2.5 nm. Sharp peaks at the center of (a) and (b) are the main peaks. They are relatively unaffected even when the mirrors have figure errors.

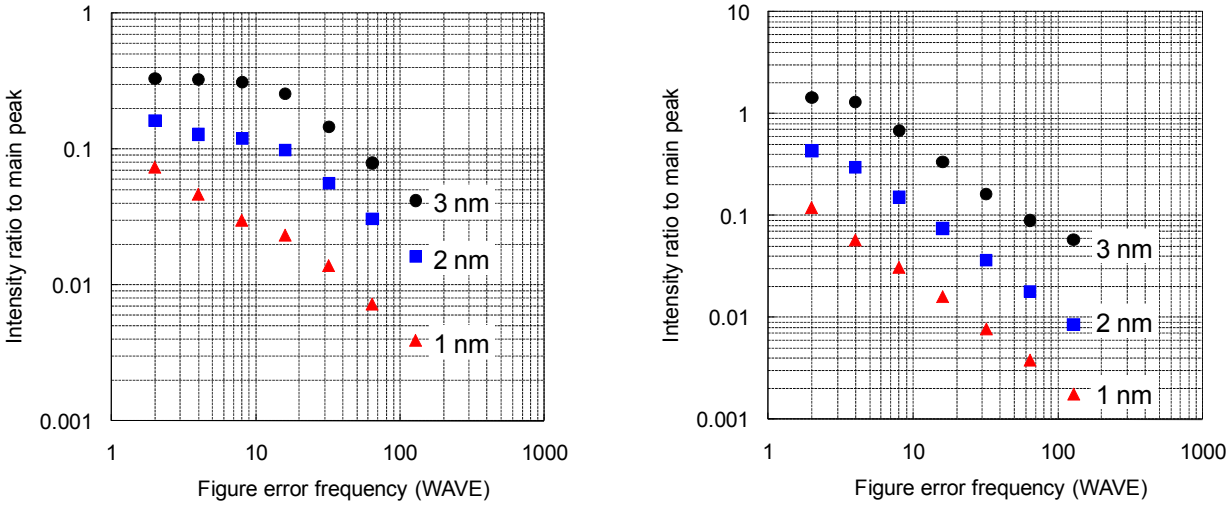

(a) On the elliptical mirror

(b) On the hyperbolic mirror

Figure 5 Relationships between spatial frequency and ratios of the intensity of the satellite peaks to the main peak for sine curves that have amplitudes of 1, 2 and 3 nm.

2.3 Fabrication of aspherical mirrors

The mirror substrates (synthetic silica) were prepared by numerically controlled elastic emission machining (NC-EEM)[8,9], microstitching interferometry (MSI)[10] and relative angle determinable stitching interferometry (RADSI)[11] with figure accuracy of better than 2 nm (Peak-to-Valley) (Fig. 6) and RMS smoothness better than 0.2 nm over an area of 64 × 48 μm^2. The figured mirrors were coated with a thin chrome binder layer and a 30-nm-thickness platinum layer using a magnetron sputtering system[12]. A beam profile calculated using the measured figure profiles and the setup described above is shown in Fig. 7. An expected minimum resolution is 43 nm in FWHM, and the heights of the satellite peaks are suppressed enough.

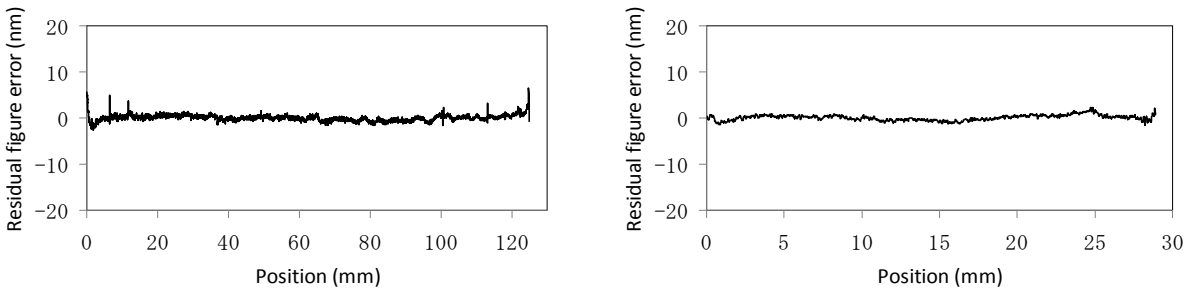

(a) Elliptical mirror

(b) Hyperbolic mirror

Figure 6 Residual figure errors on the mirror surfaces. Figured mirrors have residual figure errors of 2 nm (Peak-to-Valley) and an RMS surface roughness of 0.2 nm over an area of 64 × 48 μm^2.

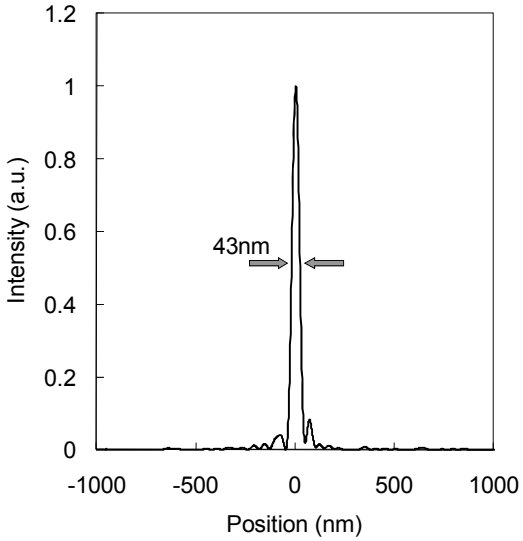

Figure 7 Beam profile calculated from the measured mirror figures. The peak has a FWHM of 43 nm. The peak means a demagnified image of a 10-μm slit installed 45 m upstream.

3. EXPERIMENTAL SETUP

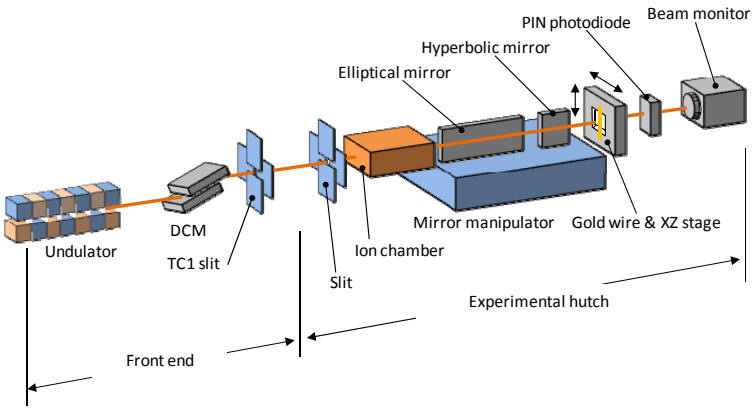

Figure 8 Experimental setup constructed to form a demagnified image in BL29XUL (EH2) of SPring-8. The TC1 slit functions as the object of the imaging system.

A schematic of the experimental setup installed in the BL29XUL (EH2) of SPring-8 is shown in Fig. 8. The quality of the demagnification image of the one-dimensional slit (TC1 slit) was evaluated. The size of the slit was set to 10 μm. X-rays generated by a standard undulator at SPring-8 are monochromatized ($\Delta E/E \approx 1.4 \times 10^{-4}$ at 11.5 keV) by a double-crystal (Si(111)) monochromator (DCM)[13]. The undulator and the DCM are set to produce 11.5 keV X-rays. The experimental hutch is located approximately 100 m downstream of the undulator and 45 m downstream of the TC1 slit. The second slit is placed just upstream of the mirrors to block X-rays coming to the outer area of the mirror. The mirrors are installed on a mirror manipulator which enables all degrees of freedom of the mirrors to be adjusted. A wire scanning method with a 200-μm-diameter gold wire and an XZ stage (Sigma Tech, FS-1050SPXY) having a positioning resolution of 1 nm was employed. A PIN photodiode was used to count transmitted X-rays. An ion chamber is placed just upstream of the mirrors to normalize the results with an incident X-ray flux.

4. RESULTS AND DISCUSSION

A demagnified image was observed with a reflectivity of 80% (in double reflection), which is in good agreement with the reflectivity calculated for an RMS surface roughness of 0.5 nm. The data acquired by the wire scanning method is shown in Fig. 9. The differential values shown in Fig. 9(b) describe a demagnified image of the slit. This demonstrates that we realized a one-dimensional Wolter mirror that has a spatial resolution of 78 nm. However, contrary to our expectations, we were unable to obtain a sharp peak approaching a diffraction-limited size of 43 nm. To consider the reason, the beam profiles with the alignment errors of the relative angle between the two mirrors were calculated. The result shown in Fig. 9(b) suggests that the relative angle was misaligned by approximately 200 μrad to the direction of increasing the angle.

The imaging characteristics were investigated by varying the glancing angle of the Wolter mirror using a tilting stage installed under the two mirrors. This is equivalent to shifting the slit position. The graph in Fig. 10 shows the relationship between the glancing angle and the FWHM; thus, the graph gives the FOV of the imaging system. As a result, the system had a much wider field than a system consisting of only the elliptical mirror. However, an expected field size of 12 μm, in which a resolution better than 50 nm is maintained, could not be obtained. In the experiment, the field size of 4.2 μm in the region of FWHMs better than 200 nm was obtained. It is thought that the degraded FOV was caused by the misalignment of the relative angle.

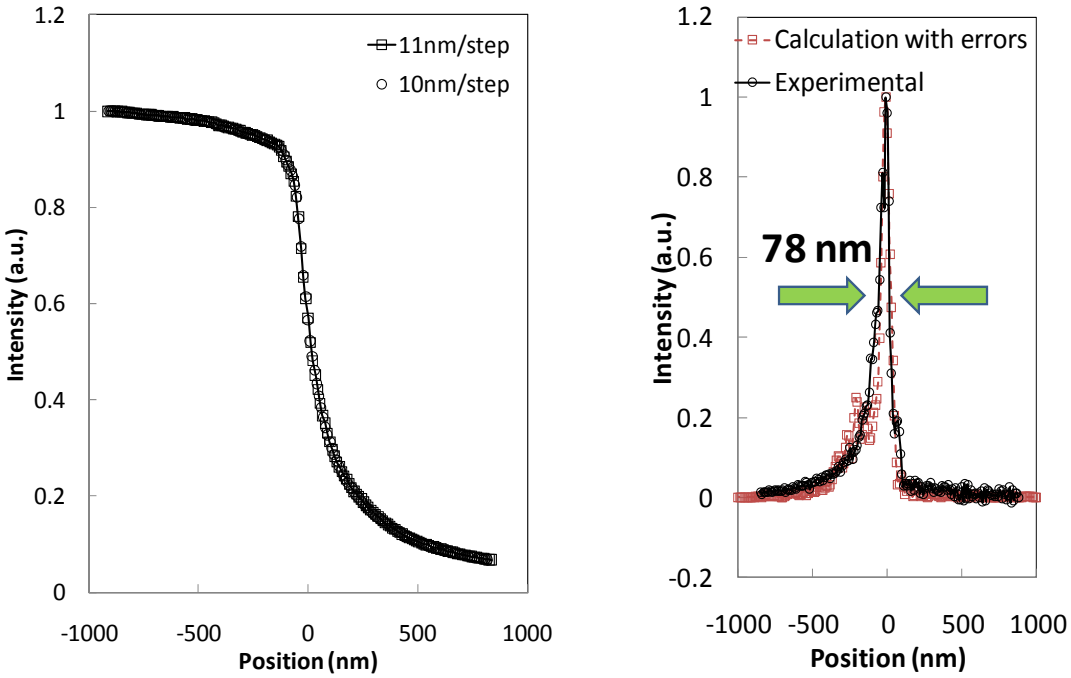

Figure 9 Results (a) acquired by wire scanning method with scanning steps of 11 and 10 nm/step and a dwell time of 1 sec/step, and (b) experimental and calculated image profiles, where the experimental results were obtained by differentiating the measured data. The dotted line in (b) was calculated with the measured mirror figures and the relative angle error of 200 μrad between the elliptical and hyperbolic mirrors. The experimental result is in good agreement with the calculated one.

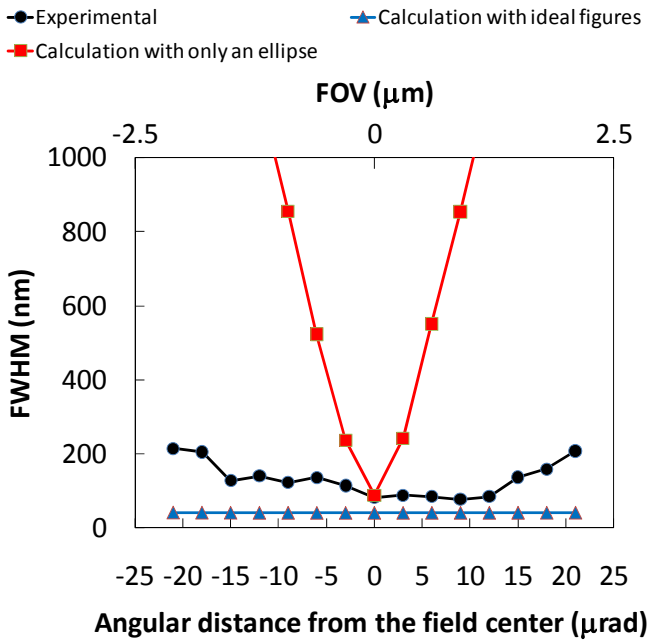

Figure 10 Relationships between the glancing angle of the Wolter mirror and the FWHM. The second horizontal axis means the FOV equivalent to the glancing angle. The line labeled "Experimental" shows the measured FWHM. The line labeled "Calculation with only an ellipse" shows the FWHM calculated for an optical setup having only the elliptical mirror.

5. CONCLUSION

A one-dimensional Wolter mirror consisting of an elliptical mirror and a hyperbolic mirror was designed and actually constructed. The best spatial resolution obtained in this study was 78 nm, which is the smallest in Wolter mirrors previously reported. Also the field size was 4.2 μm in the region of a resolution better than 200 nm.

A preliminary trial of the one-dimensional Wolter mirror suggests that a full-field hard X-ray microscope with a diffraction-limited resolution better than 50 nm without chromatic aberration can be realized. However, to realize the high-resolution microscope, difficulty in positioning four mirrors accurately has to be overcome. We are currently investigating this aspect.

ACKNOWLEDGEMENTS

This research was supported by a Grant-in-Aid for Specially Promoted Research 18002009, Grant-in-Aid for Young Scientists (B) 21700464, Global COE Program, Center for Excellence for Atomically Controlled Fabrication Technology, from the Ministry of Education, Sports, Culture, Science and Technology, Japan, and Iketani Science and Technology Foundation.

REFERENCES

[1] Y-T. Chen et al., "Full-field hard x-ray microscopy below 30 nm: a challenging nanofabrication achievement", Nanotechnology 19, 395302 (2008).
[2] H. Wolter, "Glancing Incidence Mirror Systems as Imaging Optics for X-rays", Ann. Phys. 10, 94-114 (1952).

[3] P. Kirkpatrick, A.V. Baez, "Formation of Optical Images by X-Rays", J. Opt. Soc. Am. 38, 766-774 (1948).
[4] R. Kodama et al., "Development of an advanced Kirkpatrick-Baez microscope", Optics Letters 21, 1321-1323 (1996).
[5] K. Tamasaku et al., "Pring-8 RIKEN beamline III for coherent X-ray optics", Nucl. Instrum. Methods 467, 686-689 (2001).
[6] K. Yamauchi et al., "Wave-optical evaluation of interference fringes and wavefront phase in hard X-ray beam totally reflected by mirror optics", Appl. Opt. 44, 6927-6932 (2005).
[7] S. Matsuyama et al., "Simulation study of four-mirror alignment of advanced Kirkpatrick-Baez optics", Nucl. Instrum. Methods 616, 241-245 (2010).
[8] K. Yamauchi et al., "Figuring with subnanometer-level accuracy by numerically controlled elastic emission machining", Rev. Sci. Instrum. 73, 4028-4033 (2002).
[9] K. Yamamura et al., "Fabrication of elliptical mirror at nanometer-level accuracy for hard x-ray focusing by numerically controlled plasma chemical vaporization machining", Rev. Sci. Instrum. 74, 4549-4553 (2003).
[10] K. Yamauchi et al., "Microstitching interferometry for x-ray reflective optics", Rev. Sci. Instrum. 74, 2894-2898 (2003).
[11] H. Mimura et al., "Relative angle determinable stitching interferometry for hard X-ray reflective optics", Rev. Sci. Instrum. 76, 045102 (2005).
[12] S. Handa, et al., "Highly accurate differential deposition for X-ray reflective optics", Surf. Interface Anal. 40, 1019-1022 (2008).
[13] T. Mochizuki et al., "Cryogenic cooling monochromators for the SPring-8 undualtor beamlines", Nucl. Instrum. 467, 647-649 (2001).